Tunable Late-Transition-Metal-Catalyzed Polymerization for Controlled Polymer Synthesis

Hongyi Suo [ID], Zisheng Zhang, Rui Qu, Yanan Gu and Yusheng Qin *[ID]

College of Chemistry and Chemical Engineering, Yantai University, Yantai 264005, China
* Correspondence: ysqin@ytu.edu.cn

Abstract: As a powerful protocol for the preparation of common polymers, such as polyolefins, polyesters, and polycarbonates, late-transition-metal-catalyzed polymerization can be carried out by controlling the reaction conditions or developing dynamic catalytic systems that use external stimuli to influence the performance of the active sites, resulting in well-defined polymeric materials. In particularly, under the latter conditions, 'one catalyst' can provide more than one kind of polymer with a controlled sequence from the monomer mixture, making full use of the prepared catalyst. In this review, tunable modes, including reaction conditions, redox, light or electrochemical properties, Lewis acids, and alkali metal cations, of late-transition-metal-complex (especially iron, cobalt, and nickel)-catalyzed polymerization were collected and thoroughly discussed.

Keywords: tunable polymerization; late transition metal complexes; olefin polymerization; ring-opening polymerization; ring-opening copolymerization

1. Introduction

In the past few decades, metal complexes, particularly late-transition-metal-complex-catalyzed polymerizations, such as olefin polymerization [1–11], ring-opening polymerization (ROP) [12–19], and ring-opening copolymerization (ROCOP) [20–23], have attracted considerable attention due to their high efficiency in producing polymers with predictable and well-defined structures. However, most of these polymerizations follow the "one catalyst one material" principle, whereby one catalyst produces a single type of polymer structure. In order to overcome this limitation and make full use of prepared catalysts, rational design and synthesis of polymeric materials with increasingly complicated and tailored structures have become a central focus of polymer chemistry [24,25].

Living polymerization techniques with timed monomer additions represent a new controllable method to obtain a large number of polymers with well-defined microstructures [26,27]. Although ordered monomer addition has resulted in a wide range of copolymers with basic but well-defined microstructures, this strategy appears to be overwhelmed by the increasing complexity required of modern polymers. Other strategies typically necessitate the incorporation of stimulus-responsive functional groups into well-established catalytic systems or direct modification of the intrinsic nature of the catalytically active material (i.e., oxidation state). To achieve a high degree of controllability in polymerization, delicate design of the available stimuli (e.g., mechanical force, light or electricity, redox, Lewis acids, cations, etc.) for the catalyst is required.

Recently, the emerging field of tunable/switchable catalysis, in which the chemical reactivity of a catalyst is selectively transformed between several different states (on/active and off/inactive) by changing the reaction conditions or applying an external stimulus, has provided an appealing solution to the aforementioned challenges [28–31]. Generally, reaction condition tuning, which is considered a tunable catalysis method in this review, is applicable to most polymerization reactions to control the microstructure of polymer products by changing environmental factors, such as temperature and pressure. The application

of external stimulus varies depending on specific conditions and can be categorized into reversible and irreversible forms. The former includes redox, light, and electrochemical tuning, whereby the catalyst can switch back and forth between different states; the latter includes Lewis acid and cation tuning, which can significantly alter the polymerization activity and polymer microstructure. External stimuli can be used to modify in situ reactivity and selectivity, as well as polymer molecular weight (MW), molecular weight dispersion (Đ), monomer conversion, monomer sequence, and many physical and mechanical properties, when applied to various catalytic systems [31]. Tunable polymerization methods have rapidly been extended to olefin polymerization [32–34], ROP [35–40], and ROCOP [41] catalyzed by transition metals. Tunable polymerization also affords a unique opportunity to regulate the polymer sequence and structure in a one-pot process from mixtures of monomers.

To date, there have many reviews have been conducted on the progress of tunable polymerization catalyzed by early transition metal complexes. Therefore, in this review, we summarize late transition metal polymerization (particularly iron-, cobalt-, and nickel-catalyzed olefin polymerization), as well as ROP and ROCOP via tunable methods, including reaction condition tuning, redox tuning, light or electrochemical tuning, Lewis acid tuning, and alkali metal cation tuning.

2. Reaction Condition Tuning

High activity or conversion of polymerization can be achieved by optimizing reaction conditions by changing environmental factors such as temperature, pressure, additives, or solvents. Altering these variables also has a profound impact on olefin polymerization an ring-opening (co)polymerization catalyzed by late transition metals. For instance, raising the temperature typically accelerates the chain transfer reaction, resulting in decreased MW polymers [42].

Branching is crucial in polyolefins and their copolymers because it presents a state-of-the-art topology that directly determines the properties of the polymer. Fortunately, adjusting the reaction temperature and ethylene pressure allows for fine tuning of the branching pattern. One example is how Coates and colleagues produced well-defined tetrablock polymers from ethylene alone using α-diimine nickel catalyst **1**, which responded promptly to changes in polymerization conditions (Figure 1). Linear polyethylene (PE) was formed at high pressure and low temperature (88 psi at $-35\,^\circ$C; 9/1000C), while branched PE was formed at low pressure and higher temperatures (15 psi at 20 $^\circ$C; 112/1000C) [43]. Finally, a tetrablock polymer was achieved in a one-pot reaction by alternating between two different conditions. The branches were found to be mostly methyl groups, presumably as a result of chain walking during polymerization [44,45].
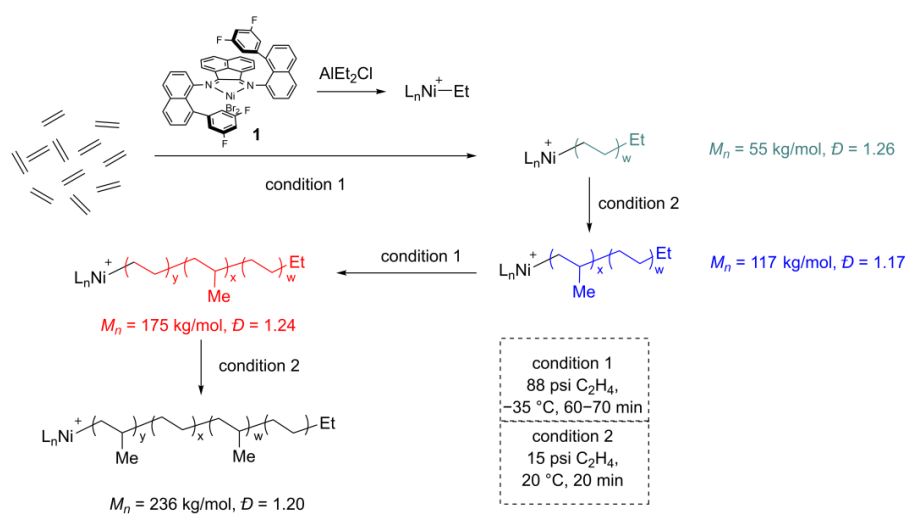
Figure 1. Synthesis of tetrablock PE by switching reaction conditions using α-diimine nickel catalyst **1**. Reprinted from Ref. [43] with permission. Copyright 2019 Royal Society of Chemistry.

Additives can also be employed to regulate the process of polymerization. Generally, polar additives are toxic reagents that used to terminate ethylene polymerization reactions, with little or no effect on the branching density of the resulting PE. However, the elegant work reported by Jian's group successfully demonstrated that palladium-promoting branching of ethylene polymerization can be drastically switched from ultra-high branching (>200/1000C, $T_g \sim -62$ °C) to significantly low branching (<10/1000C, $T_m \sim 125$ °C) when acrylonitrile is used as a polar additive (up to 4000 equivalent) [46]. In addition to failing to stop the polymerization, the addition of acrylonitrile considerably altered the branch density (importantly, without inducing chain transfer ($Đ < 1.10$)).

Controlling the polymerization process by varying the pressure is another common strategy for the preparation of CO_2-based block copolymers. For example, the Rieger group prepared terpolymers of rac-β-butyrolactone (BBL), cyclohexene oxide (CHO), and CO_2 using the one-pot method under the condition of 3 bar CO_2. On the contrary, they only obtained the copolymerization product of CHO/CO_2 when the pressure of CO_2 increased to 40 bar [47]. Chen and Pang reported a Salen-Mn^{III}-based catalyst to establish a controlled self-switching polymerization route by reversible insertion of CO_2 and achieved chemically selective ring-opening copolymerization of O-carboxylic anhydrides (OCAs) and lactide (LA) without a cocatalyst to prepare multiblock polyesters [48]. Similarly, Wang and coworkers reported a CO_2-based protection and deprotection strategy to prepare block polymers by temperature-triggered switchable ternary polymerization of epoxides/five-membered cyclic carbonates/cyclic anhydrides. The chemical protection of the conversion of epoxides to cyclic carbonates and the subsequent deprotection of cyclic carbonates to epoxides play a crucial role in the overall process, which can be controlled by temperature, i.e., epoxide/anhydride blocks at low temperatures (110 °C) and cyclic carbonate/anhydride blocks at high temperatures (180 °C) [49].

Although the method of modulating polymerization (MW, $Đ$, branch density, etc.) by reaction conditions is suitable for most catalysts and reactions, the disadvantage is that this process is slow and uncontrollable, since the heating and cooling of the reaction mixture takes time, which may lead to loss of control of the structure.

3. Redox Tuning

The use of redox to regulate polymerization can be dated back to 2003 [50]. Redox changes can significantly affect the electron distribution of complexes, allowing the reaction to switch in the "on" or "off" state. Therefore, redox has been been widely used in olefin polymerization and ring-opening polymerization since then. It has also emerged in the preparation of block copolymers by the one-pot method featuring several substrates.

BIAN (bis(imino)acenaphthene) ligands have been proven to exhibit abundant coordination chemistry with numerous metal ions (e.g., Ni and Fe) and particularly simple redox chemistry [51]. As an efficient catalyst skeleton for olefin polymerization, Ni complexes based on BIAN ligands present excellent performance in redox control of ethylene polymerization (Figure 2). Redox regulation can be achieved by adding a reductant/oxidant or by introducing ferrocene (Fc) moiety, depending on the *para*-R group.
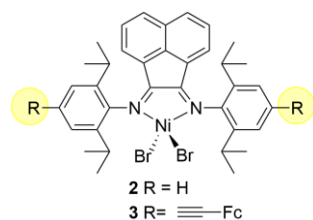
Figure 2. Redox-switchable BIAN-type catalysts (**2**–**3**).

When the R substituent is an H atom (catalyst **2**), the added reductant, CoCp$_2$ (cobaltocene), and the oxidant, AgOTf (silver trifluoromethanesulfonate), can induce a change

in the valence state and electron distribution of the nickel center in situ, which, in turn, leads to the reversible control of ethylene polymerization performance [52]. The addition of $CoCp_2$ had a more significant effect on polymerization than AgOTf, which was reflected in polymerization activity (T_m) and polymer structure (Table 1). The addition of $CoCp_2$ inhibited the "chain walking" ability of active species, resulting in a decrease in branching density as the Co/Ni ratio increased.

Table 1. Ethylene polymerization catalyzed by **2**/MAO in the presence of $CoCp_2$ or AgOTf [a]. Reprinted from Ref. [52] with permission. Copyright 2021 John Wiley and Sons.

| Entry	$CoCp_2$/Ni	AgOTf/Ni	Activity [b]	T_m/°C	Branches [c]
1	0	0	1060	−3.00	93
2	0.5	0	750	6.68	85
3	1.0	0	610	39.69	81
4	0	0.5	1020	−3.47	93
5	0	1.0	1040	−6.94	95

[a] Conditions: [Ni] = 0.0025 mmol, Al/Ni = 600, T = 20 °C, total reaction time = 15 min. [b] Activity: kg mol^{-1} h^{-1}. [c] Branching density: x/1000C.

Similarly, the Long group used a catalytic system of **2**/PMAO-IP (polyalkylaluminoxane), which can achieve precise regulation of polyethylene branching density with a $CoCp_2$ reductant (Figure 3A) [53]. With the increase in $CoCp_2$ from 0 to 1 equivalents, the degree of branching decreased by about 30%, which can be directly attributed to a decrease in the rate of β-H elimination relative to the overall rate of ethylene coordination and insertion. The microstructure of the polymer was dominated by methyl-branched chains, and with the increase in $CoCp_2$, the contents of methyl groups and long-branched chains ($\geq$6 carbon) increased. However, the MW was not significantly affected (M_w = 200–274 kg/mol). Long demonstrated that this redox-active olefin polymerization catalyst (**2**) can also be used to predictably tailor incorporation levels of polyolefin comonomers to achieve copolymerization of ethylene and higher α-olefins (Figure 3B) [54]. Once reduced by the in situ addition of $CoCp_2$, α-olefin incorporation, especially 1-hexane, is significantly reduced. This is the inverse of the previous outcome [53]. This decreasing trend can be attributed to the in situ reduction of catalyst **2**, which makes the active nickel center less electrophilic.
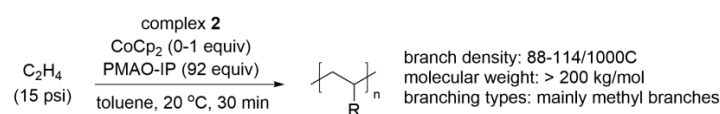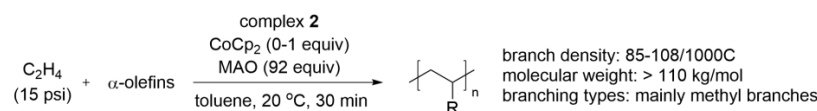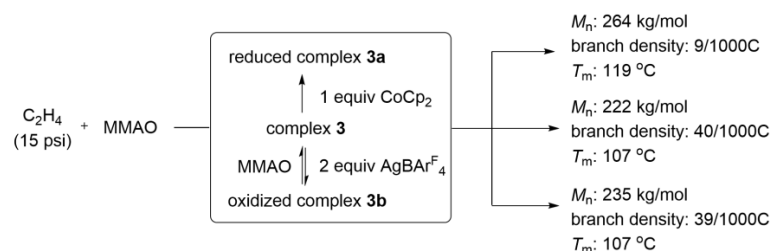

Figure 3. Redox-switchable Ni complexes (**2** and **3**) for ethylene polymerization. Reprinted from Refs. [53–55] with permission.

Ferrocene groups (Fc) incorporated into the nickel BIAN framework also created redox-tunable catalysts (catalyst **3**, Figure 3C) [55]. The reason for introducing Fc groups in the *para*-position is that they can provide additional reducing activity on the one hand and, on the other hand, reduce the degree of branching as an electron-donating group, as previously reported [56]. Complex **3** could be converted into complex **3a** or complex **3b** when exposed to CoCp$_2$ (1 equivalent) and AgBAr$^F_4$ (2 equivalents), respectively. The results show that the PE obtained by **3** and **3b** has almost the same characteristics under the same polymerization conditions. Similar to the previous example, this is due to the MAO (methylaluminoxane) reducing the Fc$^+$ (ferrocenium) substituent back to Fc (i.e., from **3b** to **3**). Conversely, **3** and **3a** yielded significantly different results, that is, **3** gave PE medium MW (M_n = 222 kg/mol) and moderate branching density (40/1000C), while **3a** gave PE medium MW (M_n = 264 kg/mol) and very low branching density (9/1000C).

A series of palladium complexes (**4**) comprising ferrocene-based phosphine–sulfonate ligands served as Chen's example of redox-controlled olefin polymerization and copolymerization (Figure 4) [57]. The transition between the neutral and oxidation states of the complexes was achieved using AgOTf and CoCp$_2$. As ethylene polymerization catalysts, both the neutral and oxidized complexes were quite effective. The branching density was somewhat increased, the MW was decreased by a factor of three to five, and the activity of the oxidized state was lowered by a factor of four to six. In contrast, the oxidized homologue showed obvious activity, while the neutral complex exhibited no activity at all in norbornene homopolymerization. A similar phenomenon was observed in complex **5**, where the oxidation state led to a decrease in activity and MW [58]. It was hypothesized that the decreased activity of oxidation states in **4** and **5** may be caused by the ligand backbone becoming more electron-withdrawing as a result of the oxidation of the ferrocene unit.
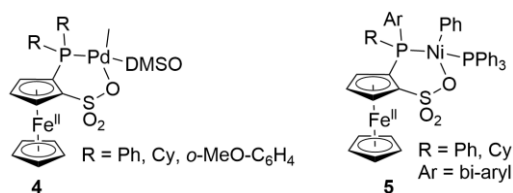

Figure 4. Phosphine–sulfonate catalyst systems.

Redox tuning also shows good control in the ROP of cyclic esters (Figure 5). FcPF$_6$ was used to reversibly transform a bis(imino)pyridine iron(II) bis(alkoxide) complex (**6a**) (Fe^{II}) into the oxidized form (**6b**) (Fe^{III}), which was then reduced back to **6a**. At room temperature for 3 h, the reduced Fe^{II} species (**6a**) catalyzed ROP of LA with 93% monomer conversion, while its oxidized Fe^{III} species (**6b**) was inert [59]. In contrast to complex **6**, pincer-type iron(II) complex **7** has exhibits catalytic activity towards ROP of ε-caprolactone (CL) in its oxidized form (**7b**) (Fe^{III}). The poly(ε-caprolactone) produced in the **7b**/alcohol system had a low Đ and exhibited a linear trend in MW with conversion [60]. Thus, ROP can occur with an in situ redox switch between "on" and "off", demonstrating the complexity of the mode of control.

In the presence of epoxide and LA monomers, a one-pot method was developed for the preparation of block copolymers, the properties of which were modulated by changing the oxidation state of the catalyst from Fe^{II} (**8a**) to Fe^{III} (**8b**). This allowed for the selective polymerization of LA and epoxide, respectively (Figure 6) [61]. One possible explanation is that while the electrophilic activation typical of an electron-deficient Fe^{III} center is more advantageous for ROCOP, the nucleophilic activation of the alkoxides is more advantageous for ROP, which is indicative of a more electron-rich Fe^{II} center. Further DFT calculations also proved this explanation [62]. A special redox-triggered crosslinking process can also be accomplished by switching between **8a** and **8b**, and the crosslinked polymer that was obtained by oxidation state **8b** showed thermal characteristics that considerably differ from those of linear polylactide [63].
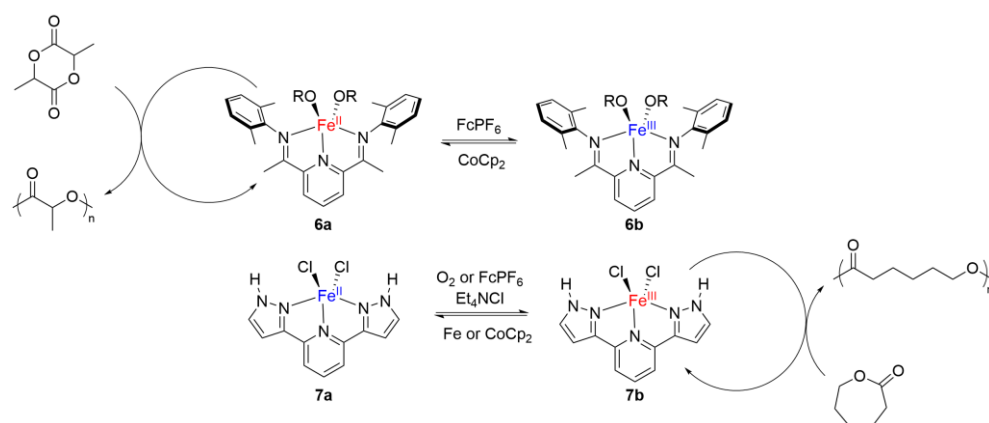
Figure 5. Redox tuning in Fe-based systems (**6** and **7**). Reprinted from Refs. [59,60] with permission. Copyright 2013 American Chemical Society, Copyright 2014 The Royal Society of Chemistry.
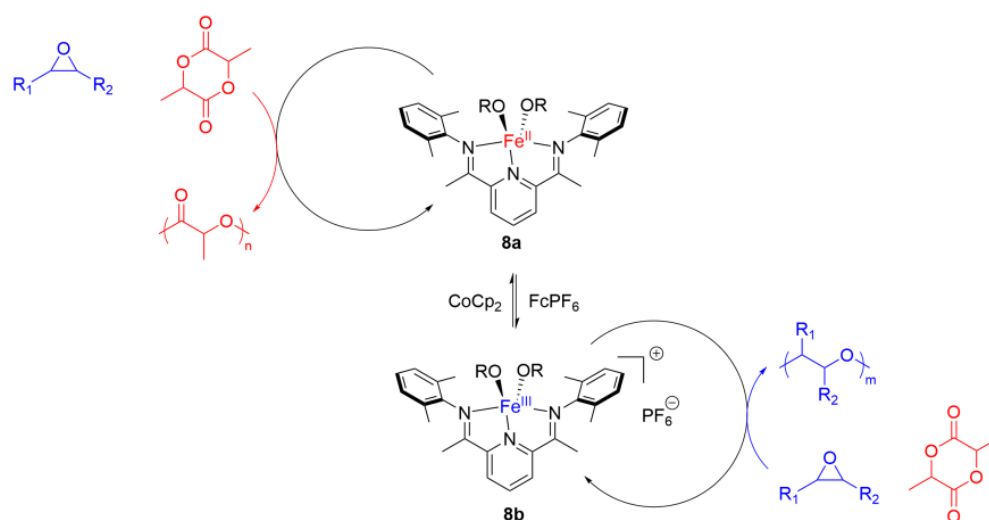
Figure 6. Redox-switchable ring-opening (co)polymerization of cyclic monomers by iron complex **8**. Reprinted from Ref. [61] with permission. Copyright 2016 John Wiley and Sons.

Three polymerization reactions—ROP of cyclic esters, ROMP (ring-opening metathesis polymerization) of cyclic olefins, and coordination-insertion polymerization of olefins—have been successfully completed using the redox-controlled method (ROMPs are not covered in the text). The redox-tuning technique has one inherent drawback in that it necessitates the external injection of oxidants and reductants, which complicates the experimental procedure, and occasionally, the catalyst or the monomer may react with the oxidizing/reducing substances. There are currently few examples of redox-controlled synthetic copolymers and a limited ability to identify monomers. It would also be exciting if redox processes could be used to alter the stereoselectivity towards the ROP of LA.

4. Electrochemical or Light Tuning

The chemical reagents (oxidants or reductants) used in the aforementioned redox tuning procedure can interact with the catalyst or the monomers, causing a loss of kinetic control of the polymerization process. In contrast, electrochemical or light control systems stand out as desirable options because they are not obtrusive and do not require any additional chemical reagents. In fact, the goal of both redox tuning, as well as electrochemical and light tuning, is to stimulate the catalyst into "on" and "off" states to achieve polymerization.

Based on redox control of lactide and epoxide copolymerization, the Byers group used electrochemical stimulation to achieve "on" and "off" states between **8a** and **8b** [64]. Without any epoxide inclusion, **8a** polymerized lactide (LA) solely from the combination of LA and cyclohexene oxide (CHO). When oxidative electrolysis was used at 3.7 V after 50% LA conversion, **8a** was oxidized into **8b**, which enabled the polymerization of CHO. Epoxide polymerization was then stopped by introducing a reducing potential of 2.3 V, converting **8b** back to **8a** and producing a clearly defined block copolymer. Furthermore, the concept mentioned above was extended to surface-initiated polymerization reactions to be used for simple surface modification [65]. The redox-switching properties and reactivity of the molecular complexes were preserved in the solid form. By using selective electrical stimulation, such a system could be used to create various polymer patterns in situ, drastically reducing the number of steps necessary to create complicated polymer designs.

Based on the chemical selectivity of different valence states of a heterometallic salen–Co–Mn complex, the Chen group established an electrochemically switchable strategy for LA, CO_2, and epoxide copolymerization that can easily synthesize polylactide (PLA) and polycarbonate (PC) multiblock copolymers [66]. The active valence of ROP of LA, which was Co^{II}-Mn^{II}, was inactive in ROCOP of CO_2 and epoxide. Co^{III}-Mn^{III}, on the other hand, was inactive in ROP and active in ROCOP (Figure 7). Electrochemical cycling between the reduction potential of −1.3 V and the oxidation potential of 1.8 V for **9** and −1.6 V and 2.1 V for **10** served to demonstrate the ability to switch the polymerization between "ON" and "OFF". The catalytic selectivity of heteronuclear complex **10** was comparable to that of **9**, but the catalytic activity was reduced, and the *Đ* values of the produced polymers were slightly higher (Table 2).
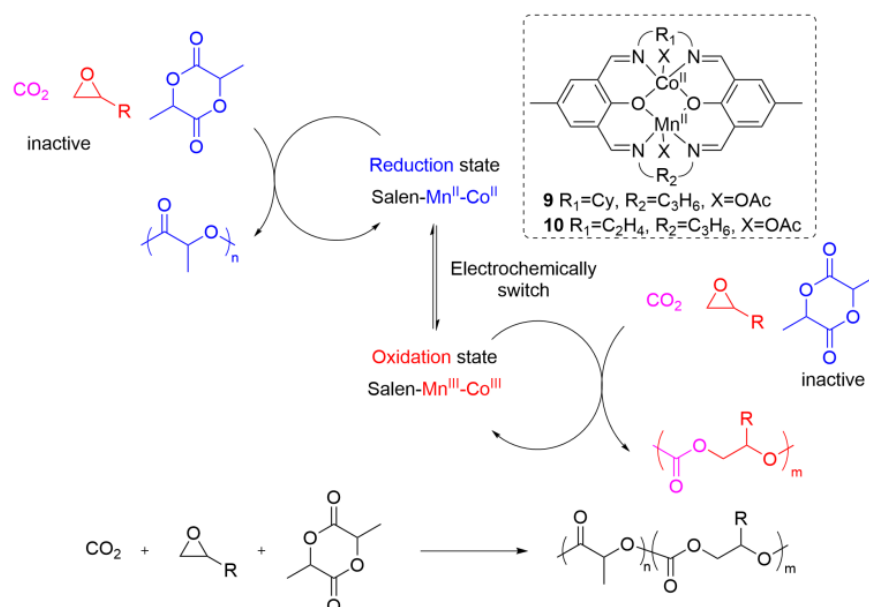
Figure 7. Electrochemically switching the catalyst reactivity in the ROP of LA and the ROCOP of CO_2 and epoxides. Reprinted from Ref. [66] with permission. Copyright 2022 John Wiley and Sons.

Table 2. Three reaction stages of LA, PO (propylene oxide), and CO_2. Reprinted from Ref. [66] with permission. Copyright 2022 John Wiley and Sons.

Reaction State	Catalyst 9		Catalyst 10	
	M_n (kg/mol)	Đ	M_n (kg/mol)	Đ
Redox state (4 h)	8.4	1.15	9.6	1.17
Oxidation state (8 h)	12.1	1.16	10.4	1.20
Redox state (4 h)	15.1	1.15	13.1	1.25

In [67], 1 atm ethylene was typically polymerized by catalyst **2** at 20 °C for 30 min in the presence of light from a 3 W blue LED and an equivalent photoreductant called *fac*-Ir(ppy)$_3$ (tris [2-phenylpyridinato-C^2, N] iridium(III)). The inclusion of *fac*-Ir(ppy)$_3$ and light irradiation (30 min) did not affect the catalytic activity of **2** but raised the polymer dispersity from 1.54 to 1.97 with the irradiation time. This pattern was seen when CoCp$_2$ was utilized as a reductant [53], indicating that *fac*-Ir(ppy)$_3$ and CoCp$_2$ may have similar functions in Ni-catalyzed ethylene polymerization. It is interesting that after polymerizing under blue LED irradiation for 30 min, the branching content of the resulting PE significantly dropped from 113/1000C to 93/1000C. This considerable decrease in PE branching density in the presence of *fac*-Ir(ppy)$_3$ is due to the delayed chain walking through decreased, more electron-rich roles in propagating Ni species during polymerization [44]. This work displays the first example of photomediated modification of the microstructure of polyethylene.
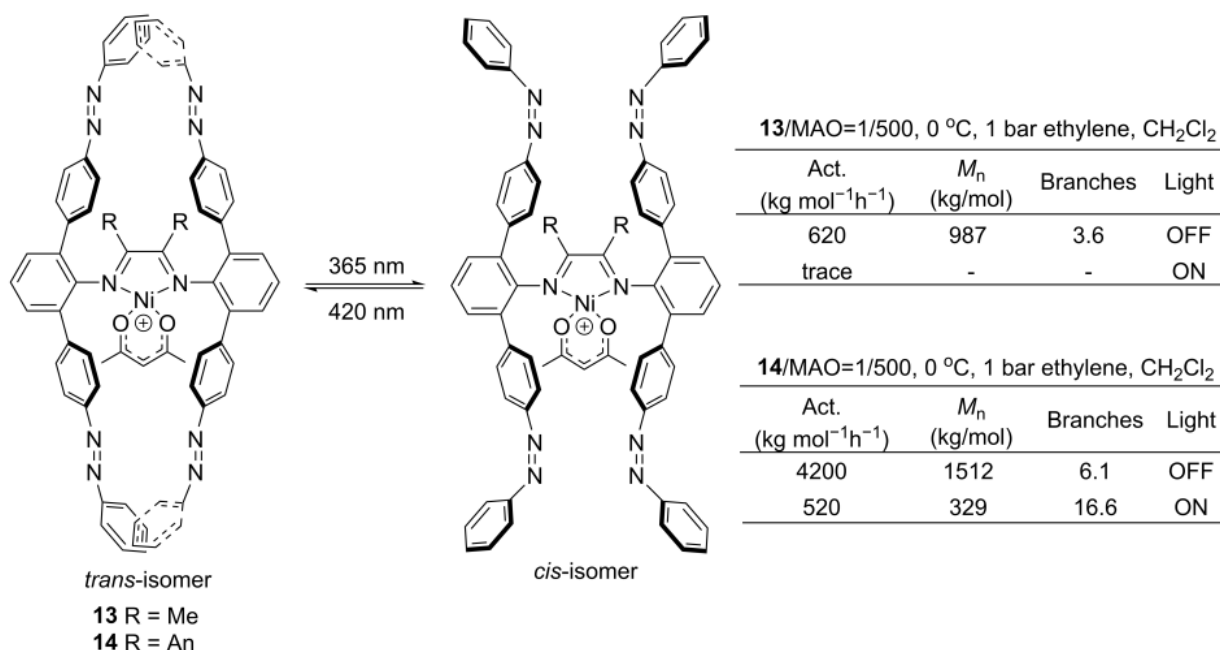
Due to the difficulty of synthesis, corresponding photoresponsive transition metal catalysts are very rare in olefin polymerization. Chen successfully reported a light-induced polymerization process in a controlled manner (Figure 8) [68]. Catalysts **11** and **12** underwent rapid and reversible photoisomerization at 365 nm or 420 nm light, i.e., cis-isomers were created when exposed to light at 365 nm, while a cis-to-trans conversion occurred when exposed to light at 420 nm. Under the same polymerization conditions, **11** exhibited distinct photoresponse characteristics, while **12** exhibited superior polymerization activity (polymerization conditions: 500 equiv. MAO, 0 °C, 8 atm ethylene, 20 mL CH$_2$Cl$_2$, 30 min). Increasing the temperature (20 °C) made the difference negligible. Contrary to **11**, **12** showed reduced activity (OFF: 33,340 kg mol^{-1} h^{-1} vs. ON: 21,140 kg mol^{-1} h^{-1}) under UV irradiation, yielding PE with a higher MW (OFF: 902 kg/mol vs. ON: 1005 kg/mol) and reduced branching density (OFF: 48/1000C vs. ON: 39/1000C). The photoinduced trans-to-cis isomerization of the azobenzene unit most likely enhanced the steric hindrance around the nickel center, according to the structure of compound **12**. This is in line with earlier research on α-diimine nickel catalysts, which showed that raising the ligand steric hindrance enhanced the MW of PE while lowering the branching density [69,70]. Additionally, catalyst **12** performed admirably when loaded with MgCl$_2$. Due to the electrical impact of photoinduced ligands, the copolymerization of ethylene with polar monomers likewise exhibited the same trend as homopolymerization.

Act. (kg mol^{-1} h^{-1})	M_n (kg/mol)	Branches	Light
100	702	16	OFF
980	421	24	ON

Act. (kg mol^{-1} h^{-1})	M_n (kg/mol)	Branches	Light
33340	902	48	OFF
21140	1005	39	ON
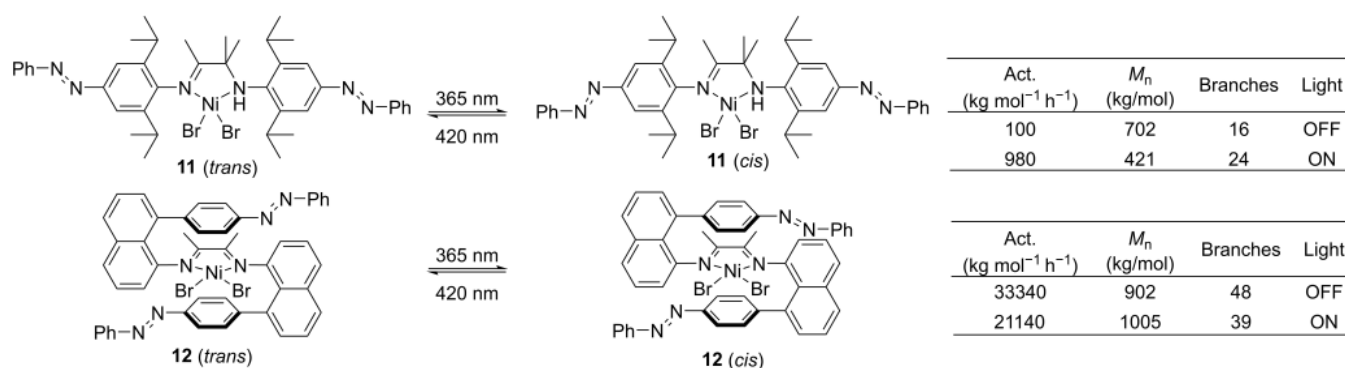
Figure 8. Polymerization data of photoresponsive nickel catalysts (**11** and **12**) at 0 °C. Reprinted from Ref. [68] with permission. Copyright 2021 John Wiley and Sons.

Jian and colleagues mounted four synergistic azobenzene moieties into symmetrical terphenyl-based α-diimine Ni(II) complexes to prepare photoresponsive catalysts **13** and **14** for ethylene polymerization and copolymerization with polar monomers, taking into account the critical role of steric hindrance shielding at the axial site [71]. Noticeably higher catalytic activities and polymer MWs and lower polymer branching densities occurred when ethylene was polymerized in the dark (Figure 9). The breakdown of the catalyst or the extremely slow chain propagation resulting from the switching of the steric hindrance may be responsible for the activity disappearing under 365 nm UV radiation. It is hypothesized

that the trans isomer state of the azobenzene in the Ni(II) catalysts existed in the dark, providing a significant steric hindrance at the axial position of the metal center. As a result, the chain transfer reaction was significantly hindered, leading to higher-molecular-weight polymers. However, significantly superior catalytic activities and polymer MWs occurred when ethylene was copolymerized with a polar monomer under UV light.


13/MAO=1/500, 0 °C, 1 bar ethylene, CH$_2$Cl$_2$

Act. (kg mol^{-1}h^{-1})	M_n (kg/mol)	Branches	Light
620	987	3.6	OFF
trace	-	-	ON

14/MAO=1/500, 0 °C, 1 bar ethylene, CH$_2$Cl$_2$

Act. (kg mol^{-1}h^{-1})	M_n (kg/mol)	Branches	Light
4200	1512	6.1	OFF
520	329	16.6	ON

trans-isomer

13 R = Me
14 R = An

cis-isomer

Figure 9. The use of azobenzene moiety in α-diimine Ni(II) catalysts (**13** and **14**) for light-tuning olefin polymerization. Reprinted from Ref. [71] with permission. Copyright 2022 John Wiley and Sons.

5. Lewis Acid Tuning

Lewis acids such boranes can also be used to tune the reactivity of metal catalysts. In 2001, Bazin and colleagues developed B(C$_6$F$_5$)$_3$-promoted olefin polymerization catalysts based on nickel α-iminocarbox-amidato complexes [72] but failed to reveal the specific role of the introduced Lewis acid [73]. Since then, several B(C$_6$F$_5$)$_3$-involved [N, O]-type Ni [74,75] and Pd catalysts [76,77] have been developed. The role of Lewis acid coordination is very similar to that of ferrocene oxidation in the aforementioned redox control system and modified conventional catalyst by substituting various ligands [78–80], reducing the electron density of the catalytically active metal center, thereby increasing the electrophilicity of the catalyst with minimal disturbance of the ligand steric hindrance, which has a considerable impact on polymerization [81–83].

The usage of borane to regulate the copolymerization of ethylene and 10-undecenoate, which was catalyzed by pyridazine–imine nickel complexes, was studied by Tan and colleagues in 2019 (Figure 10A, **15**) [84]. The authors hypothesized that boranes would bind to the free pyridazine nitrogen donor (**15b**), increasing the electrophilicity of the catalyst. The addition of BF$_3$·Et$_2$O increased catalyst activity (3 vs. 27 kg mol^{-1} h^{-1}) and decreased polymer M_n (12.2 vs. 3.2 kg/mol). Interestingly, the polymers produced by the borane-containing catalyst (**15b**) had a higher percentage of 10-undecenoate (0.6 vs. 2.0 mol%) and narrower dispersity (Đ = 8.1 vs. 2.5) than those produced by the parent catalyst (**15a**).
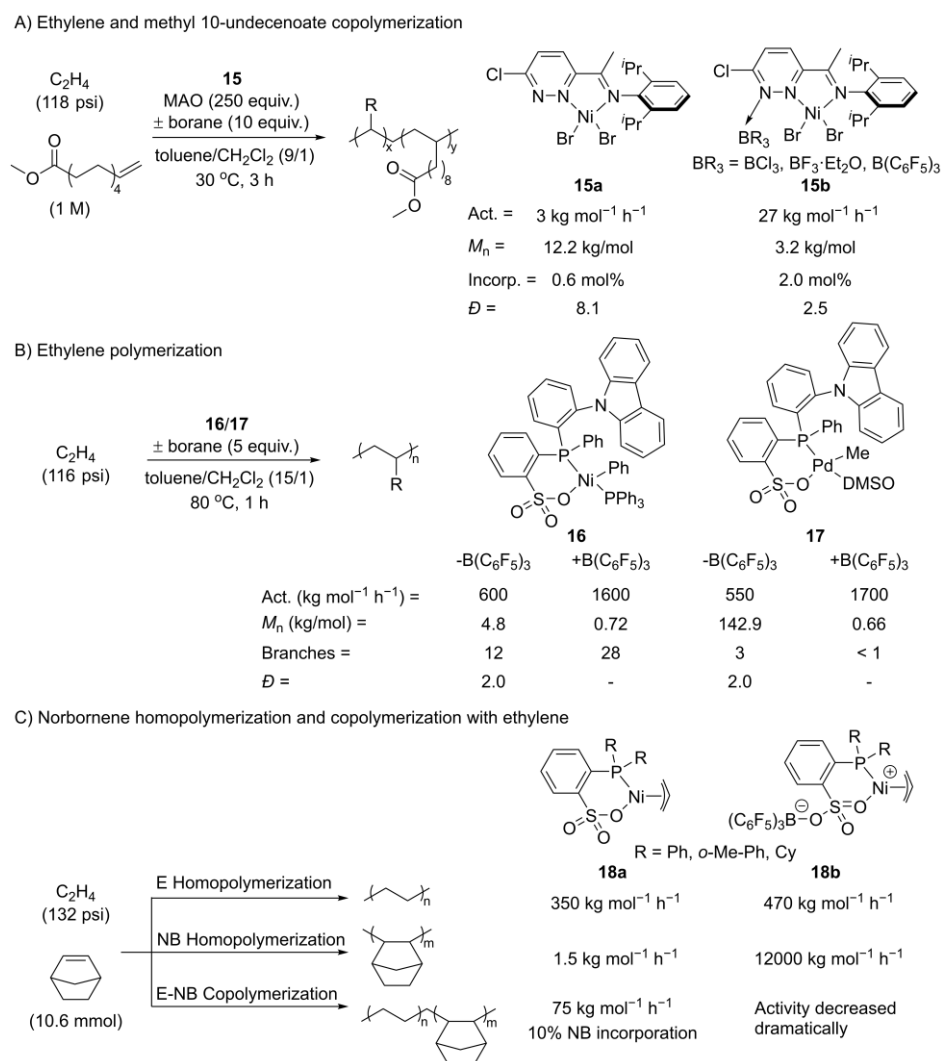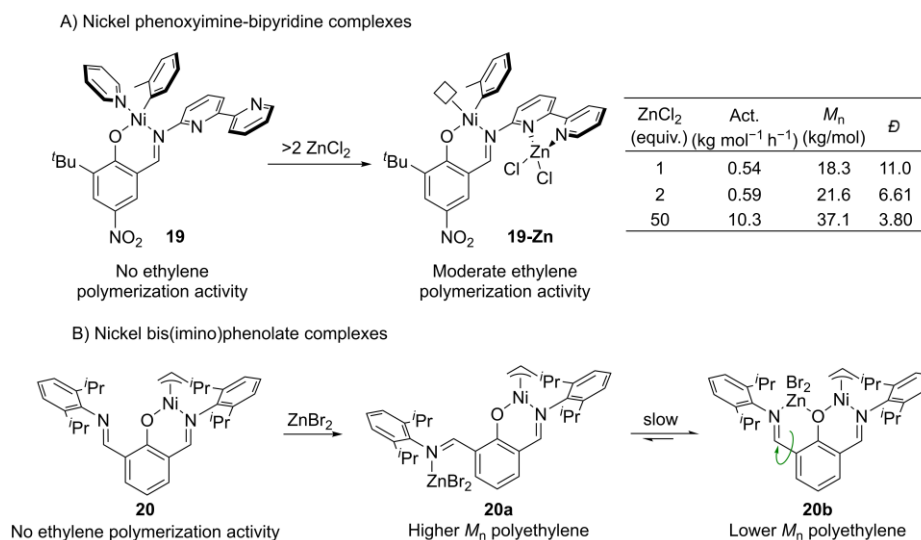
Figure 10. Ethylene (co)polymerization catalyzed by Ni/borane complexes (**15** to **18**). Reprinted from Refs. [84–86] with permission.

Lewis acid additive $B(C_6F_5)_3$ effectively increased activity and reduced polymer MW in ethylene polymerization, as reported by Chen (Figure 10B) [85]. The addition of $B(C_6F_5)_3$ to **16** resulted in an approximately 2.6-fold increase in activity accompanied by a significant decrease in MW. $B(C_6F_5)_3$ coordinated with sulfonate groups can increase the electrophilicity of the Ni center, resulting in faster chain transfer rates. The addition of $B(C_6F_5)_3$ can also effectively increase the degree of branching of the resulting polyethylene, making this strategy more widely applicable and capable of modifying the polymer structure. It was hypothesized that the ligand of $B(C_6F_5)_3$ would increase the electrophilicity of the nickel center, resulting in an increase in ligand–metal secondary interaction and an increase in branching density [87,88]. Similarly, the addition of boron salts may also promote the polymerization activity of complex **17**. Because nickel is more electrophilic than palladium, the stronger ligand–metal interactions may compete with ethylene binding, leading to a decrease in activity and polymer MW [89]. The modulation of ligand–metal secondary interactions with Lewis acid binding makes the strategy highly versatile and potentially applicable to other catalytic processes. Additionally, the direct introduction of metal Lewis acids ($Ni(OAc)_2$, $Zn(OAc)_2$, $Zn(TMEDA)(OAc)_2$) also had the potential to significantly enhance the catalytic activity of N-containing phosphonate Pd catalysts in the ethylene polymerization, producing high-molecular-weight PE (M_n = 369.2 kg/mol) and improved

catalytic activity [90]. It was demonstrated that the N-containing groups on phosphonate Pd catalysts can interact with metal Lewis acids.

Another example of the use of borane to modulate ethylene (co)polymerization was reported by the Chen group (Figure 10C) [89]. Catalyst **18a** has deficient activity in norbornene (NB) homopolymerization. The addition of one equivalent of $B(C_6F_5)_3$ to the system, i.e., **18b**, increased the catalytic activity by a factor of 4000. Compared to adding thousands of MAO equivalents, this represents a more straightforward and cost-effective activation methodology. The utilization of **18b** for ethylene homopolymerization resulted in increased activity and decreased MW, possibly due to $B(C_6F_5)_3$ binding to reduce the electron density of the nickel center. Catalyst **18a** demonstrated promising activity in the ethylene–norbornene (E-NB) copolymerization reaction, with NB incorporation of up to 10.1%. Surprisingly, the addition of $B(C_6F_5)_3$ resulted in a decrease in activity. This work represents a rare example of a late transition metal catalyst that can be used in all three types of polymerizations. The Lewis acid regulation strategy is also applicable to ROP catalyzed by zinc complexes [91].

A Lewis-acid-regulated phenoxyimide-based nickel catalyst (**19**) was reported for ethylene polymerization; the key feature of the complex is the presence of 2, 2′-bipyridine for coordination of the Lewis acid moiety (Figure 11A) [92]. Catalyst **19** was not active in ethylene polymerization but coordinated with $ZnCl_2$ to provide a discrete bimetallic nickel–zinc species (**19-Zn**) that can catalyze ethylene polymerization with low activity (50 equivalent $ZnCl_2$, 10.3 kg mol^{-1} h^{-1}). The smaller the amount of $ZnCl_2$, the greater the molecular weight distribution. Other Lewis acids (such as $CuCl_2$ and $AlCl_3$) could only produce oligomers.


Figure 11. The effect of $ZnCl_2$ additives on a series of *N*, *O*-Ni ethylene polymerization catalysts (**19** and **20**). Reprinted from Refs. [92,93] with permission.

Nickel bis(imino)phenolate complex **20** behaved significantly differently for ethylene polymerization with or without zinc salt [93]. In the absence of zinc, **20** was inactive. After adding $ZnBr_2$, bimodal PE was obtained at 35 °C, with a unimodal product obtained at 50 °C. The active species were thought to exist in two forms, i.e., **20a** and **20b**, at a low temperature of 35 °C (Figure 11B). Catalyst **20a** tended to result in high-molecular-weight PE, while **20b** resulted in low-molecular-weight products. At a high temperature of 50 °C, equilibrium favored the more thermodynamically stable formation of **20b**, so polymerization occurred mainly from this species, producing unimodal PE.

6. Alkali Metal Cation Tuning

Since the aforementioned tuning method can only convert the catalyst into two switchable states, it encounters issues such as single regulatory means and simple structural changes. Because alkali metal ions are easily soluble in organic solvents and have a wide variety of properties, including different charges, atomic radii, Lewis acidities, redox potentials, coordination geometries, etc., external alkali metal binding expands the possibilities for catalytic tuning almost infinitely.

Johnson, Brookhart, and coworkers were the first to show the advantages of combining alkali ions with olefin polymerization catalysts in 2003 (Figure 12) [94]. It was found that the activity of a nickel–lithium alkoxy phosphine complex (**22**) in the copolymerization of ethylene and hexyl acrylate was about 8.5 times higher than that of a mononickel complex (**21**). This can be interpreted as making the Ni center more electrophilic due to the direct interaction of the Li$^+$ in **22** with the nickel primary coordination sphere. Furthermore, due to the narrowed molecular weight distribution (Đ = 10.8 vs. 2.2), **22** also exhibited good controllability.
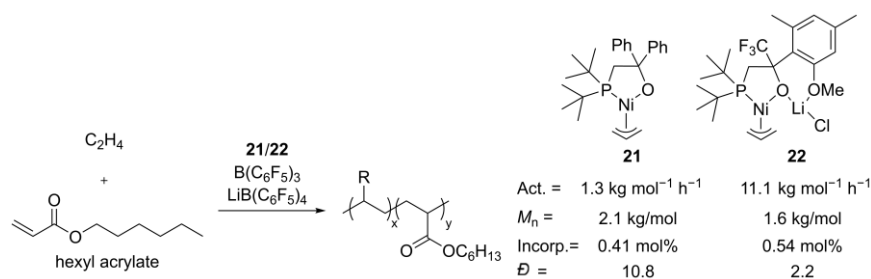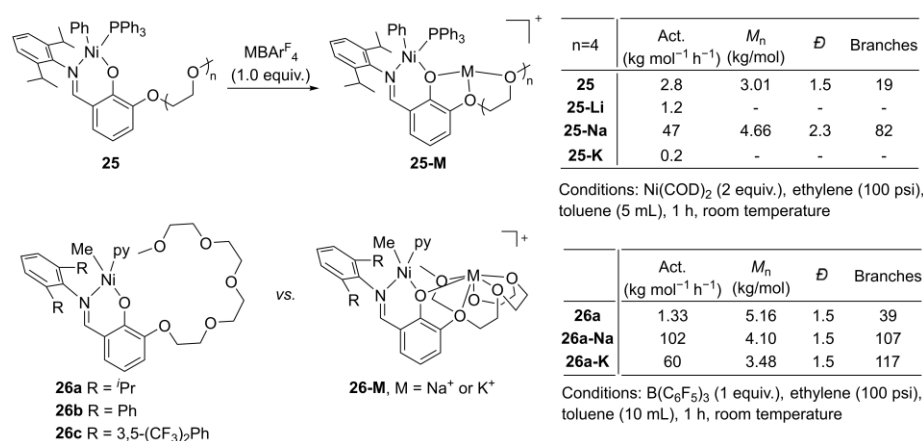

Figure 12. Lithium cation-promoted ethylene and hexyl acrylate copolymerization. Reprinted from Ref. [94] with permission. Copyright 2003 American Chemical Society.

Later, in 2016, the Tonks group also tried to control olefin polymerization using cation-tuning methods [95]. The synthesized β-oxo-δ-diimide-nickel complex has two separable, kinetically stable tautomers, such as enamine **23** and imine **24** (Figure 13). Deprotonation of **24** with M(HMDS) (where M = Li, Na and K HMDS = hexamethyldisilazide) yielded a corresponding heterobimetallic species, **24-M**. In ethylene polymerization, **24** and **24-M** produce comparable PE products with similar MW (M_n = ~12 kg/mol) and branching density (~30/1000C). The authors believe that the deprotonated catalyst (**24-M**) behaves more similarly to imine **24** than enamine **23** due to rotation. Crown ether was added to cap the alkali metal in **24-M**, ensuring that the alkali metal had no effect on the overall charge of the catalyst and therefore had little impact on the polymerization result. The authors did not explain why enamine tautomer **23** increased the branching density (118/1000C) but decreased the MW of PE (M_n = 1.6 kg/mol). These findings demonstrate the difficulties of building preorganized ligand platforms to optimize the positive impacts of secondary metals, even while cation tuning is unsuccessful in this scenario.
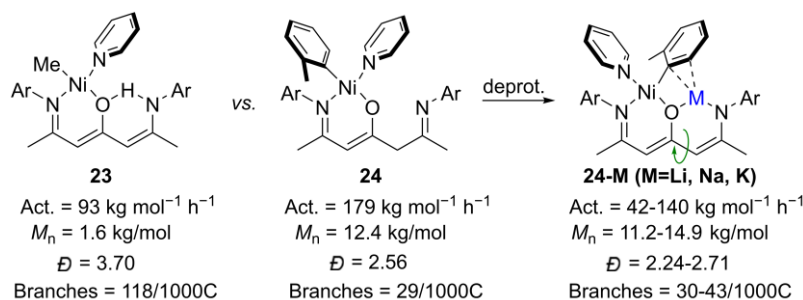
Figure 13. Nickel *N*, *O*-ligated complexes (**23** and **24**). Reprinted from Ref. [95] with permission. Copyright 2016 American Chemical Society.

The objective of the research conducted by the Do group was to examine a compound featuring two metal centers that exhibit disparate olefin polymerization characteristics. Specifically, one of the metal ions serves as a catalyst for olefin polymerization, while the other functions as an activator and binding location for polar activities [32]. This heterogeneous metal species with different active sites can enhance the coordination insertion of olefins because the bindings of the two metal centers to the monomer do not compete with one another and no sterically hindered chains of the growing polymer are located within the same catalyst structure. A series of nickel phenoxy-imine complexes containing PEG (polyethylene glycol) chains were designed and synthesized based on this concept, according to which PEG can be coordinated with alkali metal ions (M = Li, Na, K) to form bimetallic or trimetallic complexes (Figure 14) [96]. In ethylene polymerization (conditions: 2 equiv. $Ni(COD)_2$, 100 psi ethylene, 5 mL toluene, 1 h, room temperature), 25 (n = 4) exhibited low activity (2.8 kg mol^{-1} h^{-1}), and PE produced a low MW (3.0 kg/mol) and low branching density (19/1000C). The addition of alkali cations had a significant effect on polymerization, especially after the addition of Na^+ (25-Na), which significantly increased polymerization activity and the degree of product branching. The authors believe that alkali metal ions can improve the electrophilicity of nickel centers, resulting in more efficient olefin binding and insertion and a faster chain-walking rate, while bulky PEG side chains increase steric hindrance at the axial position of metal, effectively protecting the active center. This discovery served as inspiration for the development of PEG units, which interact with polar monomers to facilitate C=C double-bond coordination and influence polymerization activity, the monomer insertion rate, and copolymer MW [97,98].
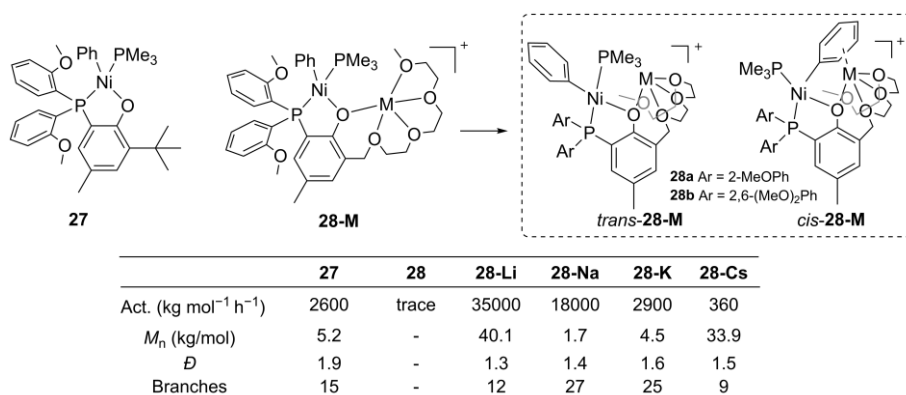

n=4	Act. (kg mol^{-1} h^{-1})	M_n (kg/mol)	Đ	Branches
25	2.8	3.01	1.5	19
25-Li	1.2	-	-	-
25-Na	47	4.66	2.3	82
25-K	0.2	-	-	-

Conditions: $Ni(COD)_2$ (2 equiv.), ethylene (100 psi), toluene (5 mL), 1 h, room temperature

	Act. (kg mol^{-1} h^{-1})	M_n (kg/mol)	Đ	Branches
26a	1.33	5.16	1.5	39
26a-Na	102	4.10	1.5	107
26a-K	60	3.48	1.5	117

Conditions: $B(C_6F_5)_3$ (1 equiv.), ethylene (100 psi), toluene (10 mL), 1 h, room temperature

Figure 14. Effect of alkali ions on ethylene polymerization by nickel phenoxy-imine complexes (25 and 26); M = Li^+, Na^+, or K^+. Reprinted from Refs. [96,99] with permission. Copyright 2015 and 2017 American Chemical Society.

Catalyst 26 was designed and synthesized on the basis of 25 and used for ethylene polymerization and copolymerization with non-polar α-olefins (Figure 14) [99]. Both alkali cation-regulated catalysts (25 and 26) required additional cocatalysts, i.e., $Ni(COD)_2$ and $B(C_6F_5)_3$, respectively. PE with different combinations of nickel catalysts and alkali metal ions (Na^+ or K^+) had different microstructures and MWs according to the findings. Higher steric hindrance 26b and 26c were more active than lower steric hindrance 26a. The activity and thermal stability of 26-M were significantly higher than those of 26. As with 25, Na^+ worked better than K^+, which was thought to be because Na^+ ions were better matched to the PEG side chain. The difficulty of logically explaining variations in polymer branching density and MW brought on by the addition of Na^+ or K^+ based on current trends emphasizes the need for a more theoretical understanding of cation-assisted coordination–insertion polymerization.

In order to further explore the regulatory mechanism of cations and realize the response of polymerization to different cations, the Do team designed and synthesized a
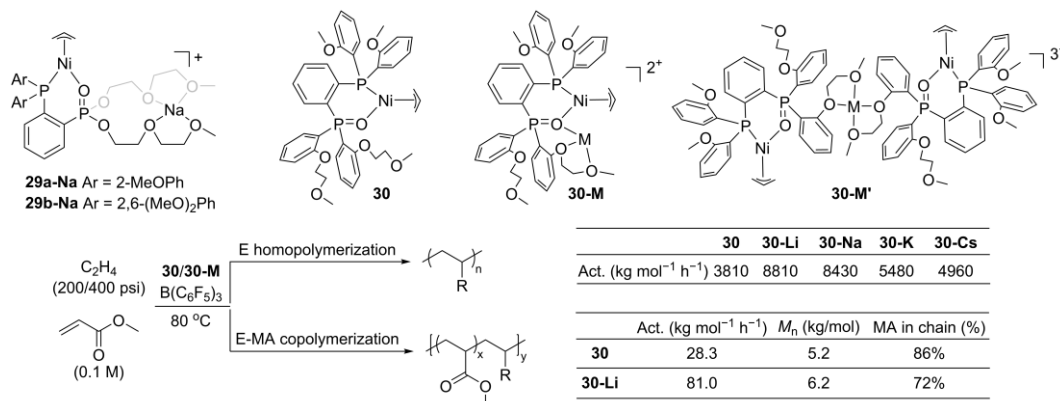
series of nickel phenoxy phosphine–PEG complexes (**27** and **28**) [100–102]. It was discovered that the steric hindrance of the catalyst met the following rule by calculating the buried volume (%V_{bur}): **27** < **28a-Na** < **28a-Li** < **28a-K** < **28a-Cs**. Therefore, the steric hindrance of the catalyst could be easily realized as long as the proper cation was chosen. Under the conditions of 30 °C, 8 equivalent Ni(COD)$_2$ (COD = 1,2,5,6-cyclooctanetetraylidene), 450 psi ethylene, toluene as solvent, and reaction for 1 h, **27** behaved moderately in ethylene polymerization (Figure 15). Although the PEG side chain also had a certain steric hindrance, catalyst **28a** was basically inactive without the coordination of alkali metal ions. The polymerization activity dramatically increased with the addition of M$^+$, and the activity was inversely correlated with the radius of the secondary metal ions; the smaller the radius, the greater the activity. Catalyst **28a-Li** is one of the most active late-transition metal catalysts reported to date. In the series of nickel–alkali species, **28a-Cs** displayed the maximum activity (23,000 kg mol^{-1} h^{-1}) at 90 °C, which we attributed to its higher thermal stability. Catalyst **28b** created a linear PE with a medium MW (M_n = 271 kg/mol) and moderate activity (279 kg mol^{-1} h^{-1}) in the absence of M$^+$. When Li$^+$, Na$^+$, K$^+$, and Cs$^+$ were added, the activity rose by 10.5, 8.6, 6.7, and 4.5, respectively. Polymerization can be accomplished in a non-switching or dynamic switching mode by varying the solvent polarity. For instance, a bimodal polymer was produced when **28a-Li** and **28a-Na** reacted with ethylene in a 100:2 combination of toluene and diethyl ether (low-polarity solvent system) because M$^+$ did not switch between nickel complexes. Catalysts **28b-C** produced a monomodal PE with Đ < 2.0 in a 98:2 mixture of toluene and diethyl ether (more polar solvent mixtures), and the MW increased with the addition of Cs$^+$ [102,103]. The experimental results show that the relative stability of the cis and trans isomers are affected by the closec distance between the secondary metal and the active center in the nickel phenoxy phosphine–PEG complex.

	27	28	28-Li	28-Na	28-K	28-Cs
Act. (kg mol^{-1} h^{-1})	2600	trace	35000	18000	2900	360
M_n (kg/mol)	5.2	-	40.1	1.7	4.5	33.9
Đ	1.9	-	1.3	1.4	1.6	1.5
Branches	15	-	12	27	25	9

Figure 15. Nickel phenoxy phosphine complexes (**27** and **28**). Reprinted from Ref. [100] with permission. Copyright 2015 American Chemical Society.

Although non-polar solvents are typically used for olefin polymerization, +2 and +3 metal cations are not soluble in them, forcing secondary metal ions to select +1 metal cations with a higher solubility. The first comprehensive examination of the magnitude of the effect of M$^+$, M^{2+}, and M^{3+} ions on the reactivity of nickel olefin polymerization catalysts was enabled by nickel phosphine phosphonate ester complexes, which can facilitate ethylene polymerization in 100% tetrahydrofuran [97]. The most effective enhancement of homopolymerization in ethylene was achieved by adding Co(OTf)$_2$ to the nickel–PEG complex (activity up to 2700 kg mol^{-1} h^{-1}). Additionally, secondary metal enhancement was observed in studies of ethylene and polar olefin (e.g., propyl vinyl ether, allyl butyl ether, methyl-10-undecenoate, and 5-acetoxy-1-pentene) copolymerization. The secondary metals in the aforementioned PEG ligated catalysts can be easily removed (e.g., by the addition of crown ethers), unlike in systems that use boranes as remote Lewis acid activators [73,84,90,104]. A similar boosting effect was also observed in Pd analogues but not as high as that in Ni complexes [105]. Although these Ni complexes in solution can form

adducts with secondary metals, the crystallographic characteristics of **29a-Na** show that the Na$^+$ is not connected to the P=O unit (Figure 16). Instead, because of its distance from the nickel center, this dangling sodium was unable to interact with it, and as a result, had no significant impact on the catalyst.

	30	30-Li	30-Na	30-K	30-Cs
Act. (kg mol^{-1} h^{-1})	3810	8810	8430	5480	4960

	Act. (kg mol^{-1} h^{-1})	M_n (kg/mol)	MA in chain (%)
30	28.3	5.2	86%
30-Li	81.0	6.2	72%

Figure 16. Bisphosphine mono-oxide ligated nickel complexes (**29** and **30**). Reprinted from Ref. [106] with permission. Copyright 2021 American Chemical Society.

To improve the catalyst design, the introduction of rigid chelated phenyl substituents helps to shorten the Ni–alkali metal distance (Figure 16, **30** and **30-M**) [106]. The reaction of **30** in solution with Li$^+$ and Na$^+$ most likely produced 1:1 and 1:1/2:1 Ni:alkali species (**30-M** and **30-M′**). Catalyst **30** showed activity up to 3810 and 28.3 kg mol^{-1} h^{-1}, making it a suitable catalysts for ethylene homopolymerization and copolymerization with methyl acrylate (MA). As previously reported, the introduction of alkali metals is beneficial for polymerization. In ethylene polymerization, the highest activity was that of **30-Li**, which was 2.3 times more active than **30**. The MW and branching density of the resultant PE were largely unaltered (M_n = 6.6–8.4 kg/mol, branches = 5–7/1000C). These findings suggest that the alkali ions played a key role in accelerating both chain growth and chain transfer rates by roughly the same order of magnitude (v$_{growth}$/v$_{transfer}$ ≈ 300). Catalyst **30-Li** showed activity up to 81.0 kg mol^{-1} h^{-1} towards ethylene copolymerization with MA. These alkali-boosted Ni-base catalysts were competitive compared to other Ni catalysts used for the copolymerization of ethylene and MA.

Low catalytic activity, poor tolerance to a large number of excess chain transfer agents, and easy byproduct generation are constraints on the production of poly(propylene carbonate) (PPC) polyols from ROCOP of CO_2 and propylene oxide (PO). A number of novel catalysts, including heterodinuclear Co(III)/M(I) macrocyclic complexes (M = Na, K, Rb, Cs, **31**), were reported by Williams (Figure 17) [107]. Two bridging phenol sites in the ligand improved the electron communication between Co(III) and M(I), increasing electronic synergy in catalysis [108,109]. These catalysts showed remarkable selectivity for polyol production (>95%), outstanding yields, and quantitative CO_2 uptake (>99%). With a turnover frequency (TOF) of 800 h^{-1} at low catalyst loading (0.25 mmol, 70 °C, 30 bar CO_2), the Co(III)/K(I) complex (**31-K**) had the maximum activity. When the radius of the alkali metal is too small, e.g., **31-Na** cannot be coordinated with PO because Na(I) may be saturated by the macrocyclic crown–ether coordination. Coplanar metal coordination within the big ring is no longer possible when the alkali metal is too large, such as Rb(I) or Cs(I), leading to the formation of aggregates. The ring opening of the potassium-coordinated epoxide by a cobalt(III) carbonate intermediate, which would be in agreement with a dinuclear process, might be the rate-determining step (RDS) that is used to explain the kinetic data. In addition to the Co(III)/K(I) complex mentioned above, the heterodinuclear Al(III)/K(I) and heterotrinuclear Zn(II)/Na(I) complexes also performed well in the ROCOP of epoxy, anhydride, and CO_2 [110,111].
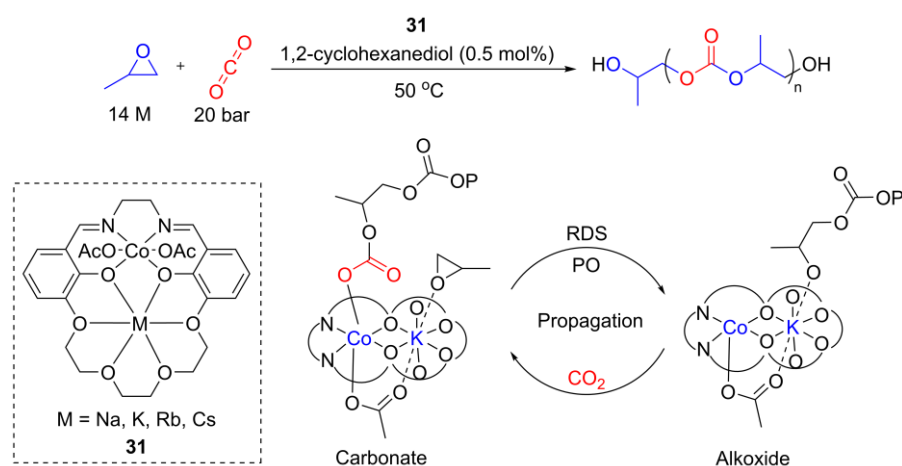
Figure 17. Heterodinuclear complexes (**31**) towards the ROCOP of CO_2 and PO.

Although there are already many reports of successful heterobimetallic catalysts (including cation tuning), creating synthetic systems that take advantage of metal–metal synergy is still a difficult task. First, the metallization of symmetric dinuclear ligands results in mixes of homobimetallic and heterobimetallic species that are challenging to distinguish, making it difficult to prepare well-structured heterobimetallic compounds [112]. Second, identification and structural determination of the synthesized heterobimetallic complexes through thorough physical characterization are not easy tasks. Finally, identifying the elements that contribute to the cooperative effect is the third obstacle in creating heterobimetallic catalysts. The radius, solubility, acidity, and alkalinity of cations influence polymerization activity, polymer MW, and microstructure in terms of cation tuning; however, the law and mechanism underlying this relationship are still unclear [113].

7. Summary and Outlook

The development of precise control of polymerization processes resulted in products with well-defined microstructures by tunable/switchable means is still in its infancy, although late-transition-metal-catalyzed polymerization to polyolefins, polyesters, and polycarbonates is now considered a relatively mature area of research. Considerable efforts have been made in the field of tunable catalysis because some earlier studies in the literature included herein clearly demonstrate that the topic is full of potential. Every tunable mode discussed in this review has advantages and disadvantages. For example, most polymerization reactions can be easily controlled by changing the reaction conditions and eliminating the requirement for special reagents. However, this regulatory process is cumbersome and difficult to implement in industrial production. Redox tuning can reversibly control polymerization processes and modify the electronic environment of the active site, although additional redox agents are needed. Light or electrochemical tuning is similar to redox tuning and can reversibly change the valence state of the metal, which has the superiority of avoiding the addition of special reagents, although it increases energy consumption. Both of these methods are deficient in controlling the stereoselectivity of the product. The electronic environment and steric hindrance effect of the catalyst can both be altered simultaneously by Lewis acid tuning; however, once bonded, the Lewis acid is challenging to remove. Due to the abundance of accessible M^{n+} salts, alkali metal cation tuning is an effective way to control the polymerization process, since it allows for the creation of numerous catalyst configurations that are not possible through the design and synthesis of ligands alone. It is challenging to build catalysts that preserve a distinct heterometallic structure in solution, have a distinctive reactivity to M^{n+} binding, and exhibit high catalytic efficiency and stability, which is a severe drawback. As a result, choosing the optimum tuning mode for a certain application necessitates consideration of a number

of variables, including whether additional additives are needed, whether it is reversible, whether it is simple to conduct, etc.

Tunable polymerization catalysis is intended to provide a more efficient method of obtaining known materials or a simple method of obtaining new materials. Tunable catalysts, which are superior to traditional catalysts, can achieve more precise control of the polymerization process, allowing for customized polymer products such as polyolefins with controlled branching density and microstructure, epoxide- and lactone-based block copolymers, etc. While significant progress has been made, some technical and chemical issues remain and need to be resolved, including high activity, polar monomer incorporation, and thermal stability, which are other challenging properties that allow for the incorporation of tunable catalysts. Furthermore, future efforts should concentrate on more sophisticated control of the system's switchable properties. For example, the development of polymerization catalysts with two distinct switching mechanisms driven by orthogonal external stimuli can be used to create complex materials with precisely tuned microstructures. As an alternative, new switchable polymeric catalysts with numerous distinct catalytic centers that may independently open and close in a selective manner can enhance the control of the polymer structure (e.g., stereoselectivity, structure, composition, topology, etc.). We anticipate that these issues will be resolved in the near future and that tunable polymerization will rank among the most reliable and effective processes for creating novel polymers.

Abbreviations

ROP	ring-opening polymerization
ROCOP	ring-opening copolymerization
PE	polyethylene
MW	molecular weight
$Đ$	molecular weight distribution
T_g	glass transition temperature
T_m	melting point
$CoCp_2$	cobaltocene
AgOTf	silver trifluoromethanesulfonate
CO_2	carbon dioxide
LA	lactide
PLA	polylactide
CHO	cyclohexene oxide
BIAN	(bis(imino)acenaphthene)
Fc	ferrocene
MAO	methylaluminoxane
M_w	weight-average molecular weight
M_n	mass-average molecular weight
ROMP	ring-opening metathesis polymerization
PEG	polyethylene glycol

References

1. Zubkevich, S.V.; Tuskaev, V.A.; Gagieva, S.C.; Bulychev, B.M. Catalytic oligomerization and polymerization of ethylene with complexes of iron triad metals: Influence of metal nature and new prospects. *Russ. Chem. Rev.* **2022**, *91*, RCR5021. [CrossRef]
2. Wu, R.; Wu, W.K.; Stieglitz, L.; Gaan, S.; Rieger, B.; Heuberger, M. Recent advances on α-diimine Ni and Pd complexes for catalyzed ethylene (co)polymerization: A comprehensive review. *Coord. Chem. Rev.* **2023**, *474*, 214844–214876. [CrossRef]
3. Deng, H.; Zheng, H.; Gao, H.; Pei, L.; Gao, H. Late transition metal catalysts with chelating amines for olefin polymerization. *Catalysts* **2022**, *12*, 936. [CrossRef]
4. Zhang, R.; Gao, R.; Gou, Q.; Lai, J.; Li, X. Recent advances in the copolymerization of ethylene with polar comonomers by nickel catalysts. *Polymers* **2022**, *14*, 3809. [CrossRef]
5. Khoshsefat, M.; Ma, Y.; Sun, W.-H. Multinuclear late transition metal catalysts for olefin polymerization. *Coord. Chem. Rev.* **2021**, *434*, 213788–213805. [CrossRef]
6. Li, P.; Yu, F.; Xu, M.; Li, X.; Li, M.; Xu, G.; Tan, C.; Zhang, S.; Wang, F. Influence of weak Fe–N bond on iron catalyzed ethylene polymerization. *Polymer* **2021**, *220*, 4626–4631. [CrossRef]
7. Qasim, M.; Bashir, M.S.; Iqbal, S.; Mahmood, Q. Recent advancements in α-diimine-nickel and -palladium catalysts for ethylene polymerization. *Eur. Polym. J.* **2021**, *160*, 110783. [CrossRef]
8. Schoeneberger, E.M.; Luinstra, G.A. Investigations on the ethylene polymerization with bisarylimine pyridine iron (BIP) catalysts. *Catalysts* **2021**, *11*, 407. [CrossRef]
9. Wang, M.; Wu, W.; Wang, X.; Huang, X.; Nai, Y.; Wei, X.; Mao, G. Research progress of iron-based catalysts for selective oligomerization of ethylene. *RSC Adv.* **2020**, *10*, 43640–43652. [CrossRef]
10. Zhong, L.; Zheng, H.; Du, C.; Du, W.; Liao, G.; Cheung, C.S.; Gao, H. Thermally robust α-diimine nickel and palladium catalysts with constrained space for ethylene (co)polymerizations. *J. Catal.* **2020**, *384*, 208–217. [CrossRef]
11. Phillips, A.M.F.; Suo, H.; Guedes da Silva, M.d.F.C.; Pombeiro, A.J.L.; Sun, W.-H. Recent developments in vanadium-catalyzed olefin coordination polymerization. *Coord. Chem. Rev.* **2020**, *416*, 213332–213360. [CrossRef]
12. Purohit, V.B.; Pięta, M.; Pietrasik, J.; Plummer, C.M. Recent advances in the ring-opening polymerization of sulfur-containing monomers. *Polym. Chem.* **2022**, *13*, 4858–4878. [CrossRef]
13. De Hoe, G.X.; Sucu, T.; Shaver, M.P. Sustainability and polyesters: Beyond metals and monomers to function and fate. *Acc. Chem. Res.* **2022**, *55*, 1514–1523. [CrossRef] [PubMed]
14. Tschan, M.J.; Gauvin, R.M.; Thomas, C.M. Controlling polymer stereochemistry in ring-opening polymerization: A decade of advances shaping the future of biodegradable polyesters. *Chem. Soc. Rev.* **2021**, *50*, 13587–13608. [CrossRef] [PubMed]
15. Jia, Z.W.; Li, Y.J.; Wu, J.C. Sequence-controlled alternating copolyesters synthesis via selective ring-opening polymerization. *Macromol. Chem. Phys.* **2021**, *222*, 2100323. [CrossRef]
16. Schafer, P.M.; Herres-Pawlis, S. Robust guanidine metal catalysts for the ring-opening polymerization of lactide under industrially relevant conditions. *ChemPlusChem* **2020**, *85*, 1044–1052. [CrossRef]
17. Santoro, O.; Zhang, X.; Redshaw, C. Synthesis of biodegradable polymers: A review on the use of schiff-base metal complexes as catalysts for the ring opening polymerization (ROP) of cyclic esters. *Catalysts* **2020**, *10*, 800. [CrossRef]
18. Petrus, R.; Sobota, P. Magnesium and zinc alkoxides and aryloxides supported by commercially available ligands as promoters of chemical transformations of lactic acid derivatives to industrially important fine chemicals. *Coord. Chem. Rev.* **2019**, *396*, 72–88. [CrossRef]
19. Nifant'ev, I.; Ivchenko, P. Coordination ring-opening polymerization of cyclic esters: A critical overview of dft modeling and visualization of the reaction mechanisms. *Molecules* **2019**, *24*, 4117. [CrossRef]
20. Plajer, A.J.; Williams, C.K. Heterocycle/heteroallene ring-opening copolymerization: Selective catalysis delivering alternating copolymers. *Angew. Chem. Int. Ed.* **2022**, *61*, e202104495. [CrossRef]
21. Lidston, C.A.L.; Severson, S.M.; Abel, B.A.; Coates, G.W. Multifunctional catalysts for ring-opening copolymerizations. *ACS Catal.* **2022**, *22*, 11037–11070. [CrossRef]
22. Diment, W.T.; Lindeboom, W.; Fiorentini, F.; Deacy, A.C.; Williams, C.K. Synergic heterodinuclear catalysts for the ring-opening copolymerization (ROCOP) of epoxides, carbon dioxide, and anhydrides. *Acc. Chem. Res.* **2022**, *55*, 1997–2010. [CrossRef] [PubMed]
23. Darensbourg, D.J. Switchable catalytic processes involving the copolymerization of epoxides and carbon dioxide for the preparation of block polymers. *Inorg. Chem. Front.* **2017**, *4*, 412–419. [CrossRef]
24. Matyjaszewski, K. Macromolecular engineering: From rational design through precise macromolecular synthesis and processing to targeted macroscopic material properties. *Prog. Polym. Sci.* **2005**, *30*, 858–875. [CrossRef]
25. Walsh, D.J.; Hyatt, M.G.; Miller, S.A.; Guironnet, D. Recent trends in catalytic polymerizations. *ACS Catal.* **2019**, *9*, 11153–11188. [CrossRef]
26. Webster, O.W. Living polymerization methods. *Science* **1991**, *251*, 887–893. [CrossRef]
27. Yagci, Y.; Atilla Tasdelen, M. Mechanistic transformations involving living and controlled/living polymerization methods. *Prog. Polym. Sci.* **2006**, *31*, 1133–1170. [CrossRef]
28. Doerr, A.M.; Burroughs, J.M.; Gitter, S.R.; Yang, X.; Boydston, A.J.; Long, B.K. Advances in polymerizations modulated by external stimuli. *ACS Catal.* **2020**, *10*, 14457–14515. [CrossRef]
29. Blanco, V.; Leigh, D.A.; Marcos, V. Artificial switchable catalysts. *Chem. Soc. Rev.* **2015**, *44*, 5341–5370. [CrossRef]

30. Teator, A.J.; Lastovickova, D.N.; Bielawski, C.W. Switchable polymerization catalysts. *Chem. Rev.* **2016**, *116*, 1969–1992. [CrossRef]
31. Leibfarth, F.A.; Mattson, K.M.; Fors, B.P.; Collins, H.A.; Hawker, C.J. External regulation of controlled polymerizations. *Angew. Chem. Int. Ed.* **2013**, *52*, 199–210. [CrossRef]
32. Tran, T.V.; Do, L.H. Tunable modalities in polyolefin synthesis via coordination insertion catalysis. *Eur. Polym. J.* **2021**, *142*, 110100–110114. [CrossRef]
33. Tan, C.; Chen, M.; Chen, C. 'Catalyst + x' strategies for transition metal-catalyzed olefin-polar monomer copolymerization. *Trends Chem.* **2023**, *5*, 147–159. [CrossRef]
34. Kaiser, J.M.; Long, B.K. Recent developments in redox-active olefin polymerization catalysts. *Coord. Chem. Rev.* **2018**, *372*, 141–152. [CrossRef]
35. Chen, C. Redox-controlled polymerization and copolymerization. *ACS Catal.* **2018**, *8*, 5506–5514. [CrossRef]
36. Wei, J.; Diaconescu, P.L. Redox-switchable ring-opening polymerization with ferrocene derivatives. *Acc. Chem. Res.* **2019**, *52*, 415–424. [CrossRef]
37. Chen, M.; Chen, C. Controlling the ring-opening polymerization process using external stimuli. *Chin. J. Chem.* **2020**, *38*, 282–286. [CrossRef]
38. Kaler, S.; Jones, M.D. Recent advances in externally controlled ring-opening polymerisations. *Dalton Trans.* **2022**, *51*, 1241–1256. [CrossRef] [PubMed]
39. Shawver, N.M.; Doerr, A.M.; Long, B.K. A perspective on redox-switchable ring-opening polymerization. *J. Poly. Sci.* **2022**, *1*, 361–371. [CrossRef]
40. Li, B.; Hu, C.; Pang, X.; Chen, X. Valence-variable catalysts for redox-controlled switchable ring-opening polymerization. *Chem. Asian J.* **2023**, *18*, e202201031. [CrossRef] [PubMed]
41. Deacy, A.C.; Gregory, G.L.; Sulley, G.S.; Chen, T.T.D.; Williams, C.K. Sequence control from mixtures: Switchable polymerization catalysis and future materials applications. *J. Am. Chem. Soc.* **2021**, *143*, 10021–10040. [CrossRef]
42. Zhang, Y.; Kang, X.; Jian, Z. Selective branch formation in ethylene polymerization to access precise ethylene-propylene copolymers. *Nat. Commun.* **2022**, *13*, 725. [CrossRef] [PubMed]
43. Padilla-Velez, O.; O'Connor, K.S.; LaPointe, A.M.; MacMillan, S.N.; Coates, G.W. Switchable living nickel(II) α-diimine catalyst for ethylene polymerisation. *Chem. Commun.* **2019**, *55*, 7607–7610. [CrossRef] [PubMed]
44. Guo, L.; Dai, S.; Sui, X.; Chen, C. Palladium and nickel catalyzed chain walking olefin polymerization and copolymerization. *ACS Catal.* **2016**, *6*, 428–441. [CrossRef]
45. Guan, Z.; Cotts, P.M.; McCord, E.F.; McLain, S.J. Chain walking: A new strategy to control polymer topology. *Science* **1999**, *283*, 2059–2062. [CrossRef]
46. Zhang, Y.; Jian, Z. Polar additive triggered branching switch and block polyolefin topology in living ethylene polymerization. *Macromolecules* **2021**, *54*, 3191–3196. [CrossRef]
47. Kernbichl, S.; Reiter, M.; Adams, F.; Vagin, S.; Rieger, B. CO_2-controlled one-pot synthesis of AB, ABA block, and statistical terpolymers from β-butyrolactone, epoxides, and CO_2. *J. Am. Chem. Soc.* **2017**, *139*, 6787–6790. [CrossRef]
48. Huang, Y.; Hu, C.; Zhou, Y.; Duan, R.; Sun, Z.; Wan, P.; Xiao, C.; Pang, X.; Chen, X. Monomer controlled switchable copolymerization: A feasible route for the functionalization of poly(lactide). *Angew. Chem. Int. Ed.* **2021**, *60*, 9274–9278. [CrossRef]
49. You, H.; Zhuo, C.; Yan, S.; Wang, E.; Cao, H.; Liu, S.; Wang, X. CO_2 deprotection-mediated switchable polymerization for precise construction of block copolymers. *Macromolecules* **2022**, *55*, 10980–10992. [CrossRef]
50. Gibson, V.C.; Halliwell, C.M.; Long, N.J.; Oxford, P.J.; Smith, A.M.; White, A.J.P.; Williams, D.J. Synthetic, spectroscopic and olefin oligomerisation studies on nickel and palladium complexes containing ferrocene substituted nitrogen donor ligands. *Dalton Trans.* **2003**, *5*, 918–926. [CrossRef]
51. Bernauer, J.; Polker, J.; Jacobi von Wangelin, A. Redox-active bian-based diimine ligands in metal-catalyzed small molecule syntheses. *ChemCatChem* **2022**, *14*, e202101182. [CrossRef] [PubMed]
52. Xing, Y.; Yu, H.; Wang, L.; Wang, N.; Zhu, L.; Liang, R. The formation of polyethylene using α-diiminonickel precatalyst in the presence of $CoCp_2$ and AgOTf. *ChemistrySelect* **2021**, *6*, 7663–7669. [CrossRef]
53. Anderson, W.C., Jr.; Rhinehart, J.L.; Tennyson, A.G.; Long, B.K. Redox-active ligands: An advanced tool to modulate polyethylene microstructure. *J. Am. Chem. Soc.* **2016**, *138*, 774–777. [CrossRef]
54. Anderson, W.C.; Long, B.K. Modulating polyolefin copolymer composition via redox-active olefin polymerization catalysts. *ACS Macro Lett.* **2016**, *5*, 1029–1033. [CrossRef] [PubMed]
55. Anderson, W.C.; Park, S.H.; Brown, L.A.; Kaiser, J.M.; Long, B.K. Accessing multiple polyethylene grades via a single redox-active olefin polymerization catalyst. *Inorg. Chem. Front.* **2017**, *4*, 1108–1112. [CrossRef]
56. Popeney, C.; Guan, Z. Ligand electronic effects on late transition metal polymerization catalysts. *Organometallics* **2005**, *24*, 1145–1155. [CrossRef]
57. Chen, M.; Yang, B.; Chen, C. Redox-controlled olefin (co)polymerization catalyzed by ferrocene-bridged phosphine-sulfonate palladium complexes. *Angew. Chem. Int. Ed.* **2015**, *54*, 15520–15524. [CrossRef]
58. Yang, B.; Pang, W.; Chen, M. Redox control in olefin polymerization catalysis by phosphine–sulfonate palladium and nickel complexes. *Eur. J. Inorg. Chem.* **2017**, *2017*, 2510–2514. [CrossRef]
59. Biernesser, A.B.; Li, B.; Byers, J.A. Redox-controlled polymerization of lactide catalyzed by bis(imino)pyridine iron bis(alkoxide) complexes. *J. Am. Chem. Soc.* **2013**, *135*, 16553–16560. [CrossRef]

60. Fang, Y.Y.; Gong, W.J.; Shang, X.J.; Li, H.X.; Gao, J.; Lang, J.P. Synthesis and structure of a ferric complex of 2,6-di(1H-pyrazol-3-yl)pyridine and its excellent performance in the redox-controlled living ring-opening polymerization of ε-caprolactone. *Dalton Trans.* **2014**, *43*, 8282–8289. [CrossRef]

61. Biernesser, A.B.; Delle Chiaie, K.R.; Curley, J.B.; Byers, J.A. Block copolymerization of lactide and an epoxide facilitated by a redox switchable iron-based catalyst. *Angew. Chem. Int. Ed.* **2016**, *55*, 5251–5254. [CrossRef] [PubMed]

62. Xu, X.; Lu, H.; Luo, G.; Kang, X.; Luo, Y. Theoretical insight into the opposite redox activity of iron complexes toward the ring opening polymerization of lactide and epoxide. *Inorg. Chem. Front.* **2021**, *8*, 1005–1014. [CrossRef]

63. Delle Chiaie, K.R.; Yablon, L.M.; Biernesser, A.B.; Michalowski, G.R.; Sudyn, A.W.; Byers, J.A. Redox-triggered crosslinking of a degradable polymer. *Polym. Chem.* **2016**, *7*, 4675–4681. [CrossRef]

64. Qi, M.; Dong, Q.; Wang, D.; Byers, J.A. Electrochemically switchable ring-opening polymerization of lactide and cyclohexene oxide. *J. Am. Chem. Soc.* **2018**, *140*, 5686–5690. [CrossRef]

65. Qi, M.; Zhang, H.; Dong, Q.; Li, J.; Musgrave, R.A.; Zhao, Y.; Dulock, N.; Wang, D.; Byers, J.A. Electrochemically switchable polymerization from surface-anchored molecular catalysts. *Chem. Sci.* **2021**, *12*, 9042–9052. [CrossRef] [PubMed]

66. Huang, Y.; Hu, C.; Pang, X.; Zhou, Y.; Duan, R.; Sun, Z.; Chen, X. Electrochemically controlled switchable copolymerization of lactide, carbon dioxide, and epoxides. *Angew. Chem. Int. Ed.* **2022**, *61*, e202202660. [CrossRef]

67. Kaiser, J.M.; Anderson, W.C.; Long, B.K. Photochemical regulation of a redox-active olefin polymerization catalyst: Controlling polyethylene microstructure with visible light. *Polym. Chem.* **2018**, *9*, 1567–1570. [CrossRef]

68. Peng, D.; Chen, C. Photoresponsive palladium and nickel catalysts for ethylene polymerization and copolymerization. *Angew. Chem. Int. Ed.* **2021**, *60*, 22195–22200. [CrossRef]

69. Gong, Y.; Li, S.; Gong, Q.; Zhang, S.; Liu, B.; Dai, S. Systematic investigations of ligand steric effects on α-diimine nickel catalyzed olefin polymerization and copolymerization. *Organometallics* **2019**, *38*, 2919–2926. [CrossRef]

70. Muhammad, Q.; Tan, C.; Chen, C. Concerted steric and electronic effects on α-diimine nickel- and palladium-catalyzed ethylene polymerization and copolymerization. *Sci. Bull.* **2020**, *65*, 300–307. [CrossRef] [PubMed]

71. Yang, J.; Hu, X.; Jian, Z. Photoresponsive α-diimine nickel modulated ethylene (co)polymerization. *Chin. J. Chem.* **2022**, *40*, 2919–2926. [CrossRef]

72. Lee, B.Y.; Bazan, G.C.; Vela, J.; Komon, Z.J.; Bu, X. Alpha-iminocarboxamidato-nickel(II) ethylene polymerization catalysts. *J. Am. Chem. Soc.* **2001**, *123*, 5352–5353. [CrossRef]

73. Chen, Y.; Boardman, B.M.; Wu, G.; Bazan, G.C. A zwitterionic nickel–olefin initiator for the preparation of high molecular weight polyethylene. *J. Organomet. Chem.* **2007**, *692*, 4745–4749. [CrossRef]

74. Shim, C.B.; Kim, Y.H.; Lee, B.Y.; Dong, Y.; Yun, H. [2-(alkylideneamino)benzoato]nickel(II) complexes: Active catalysts for ethylene polymerization. *Organometallics* **2003**, *22*, 4272–4280. [CrossRef]

75. Chen, Y.; Wu, G.; Bazan, G.C. Remote activation of nickel catalysts for ethylene oligomerization. *Angew. Chem. Int. Ed.* **2005**, *44*, 1108–1112. [CrossRef]

76. Cai, Z.; Shen, Z.; Zhou, X.; Jordan, R.F. Enhancement of chain growth and chain transfer rates in ethylene polymerization by (phosphine-sulfonate)PdMe catalysts by binding of $B(C_6F_5)_3$ to the sulfonate group. *ACS Catal.* **2012**, *2*, 1187–1195. [CrossRef]

77. Contrella, N.D.; Jordan, R.F. Lewis acid modification and ethylene oligomerization behavior of palladium catalysts that contain a phosphine-sulfonate-diethyl phosphonate ancillary ligand. *Organometallics* **2014**, *33*, 7199–7208. [CrossRef]

78. Xie, K.; Xu, S.; Hao, W.; Wang, J.; Huang, A.; Zhang, Y. Surface effect of the mgcl2 support in Ziegler–Natta catalyst for ethylene polymerization: A computational study. *Appl. Surf. Sci.* **2022**, *589*, 153002. [CrossRef]

79. Xie, K.; Xu, J.; Liu, P. Effect of ligands in $TiCl_3(OAr)$ catalysts for ethylene polymerization: Computational and experimental studies. *Appl. Surf. Sci.* **2018**, *461*, 175–181. [CrossRef]

80. Xie, K.; Hao, W.; Xu, S.; Wang, J.; Wang, X.; Han, Z. Substituent effect of Cp_2TiCl_2 catalyst for ethylene polymerization: A DFT study. *Polyolefins J.* **2023**, *10*, 35–43. [CrossRef]

81. Kuhn, P.; Semeril, D.; Matt, D.; Chetcuti, M.J.; Lutz, P. Structure-reactivity relationships in SHOP-type complexes: Tunable catalysts for the oligomerisation and polymerisation of ethylene. *Dalton Trans.* **2007**, *5*, 515–528. [CrossRef]

82. Komon, Z.J.A.; Bu, X.; Bazan, G.C. Synthesis of butene−ethylene and hexene−butene−ethylene copolymers from ethylene via tandem action of well-defined homogeneous catalysts. *J. Am. Chem. Soc.* **2000**, *122*, 1830–1831. [CrossRef]

83. Komon, Z.J.A.; Bu, X.; Bazan, G.C. Synthesis, characterization, and ethylene oligomerization action of $[(C_6H_5)_2PC_6H_4C(O-B(C_6F_5)_3)O-\kappa^2P,O]Ni(\eta^3-CH_2C_6H_5)$. *J. Am. Chem. Soc.* **2000**, *122*, 12379–12380. [CrossRef]

84. Wang, G.; Li, M.; Pang, W.; Chen, M.; Tan, C. Lewis acids in situ modulate pyridazine-imine Ni catalysed ethylene (co)polymerisation. *New J. Chem.* **2019**, *43*, 13630–13634. [CrossRef]

85. Tan, C.; Qasim, M.; Pang, W.; Chen, C. Ligand–metal secondary interactions in phosphine–sulfonate palladium and nickel catalyzed ethylene (co)polymerization. *Polym. Chem.* **2020**, *11*, 411–416. [CrossRef]

86. Chen, M.; Zou, W.; Cai, Z.; Chen, C. Norbornene homopolymerization and copolymerization with ethylene by phosphine-sulfonate nickel catalysts. *Polym. Chem.* **2015**, *6*, 2669–2676. [CrossRef]

87. Falivene, L.; Wiedemann, T.; Gottker-Schnetmann, I.; Caporaso, L.; Cavallo, L.; Mecking, S. Control of chain walking by weak neighboring group interactions in unsymmetrical catalysts. *J. Am. Chem. Soc.* **2018**, *140*, 1305–1312. [CrossRef]

88. Schiebel, E.; Santacroce, S.; Falivene, L.; Göttker-Schnetmann, I.; Caporaso, L.; Mecking, S. Tailored strength neighboring group interactions switch polymerization to dimerization catalysis. *ACS Catal.* **2019**, *9*, 3888–3894. [CrossRef]

89. Li, M.; Wang, X.; Luo, Y.; Chen, C. A second-coordination-sphere strategy to modulate nickel- and palladium-catalyzed olefin polymerization and copolymerization. *Angew. Chem. Int. Ed.* **2017**, *56*, 11604–11609. [CrossRef]

90. Wang, Y.; Pang, W.; Zhang, S.; Tan, C. Lewis acids modulation in phosphine-sulfonate palladium catalyzed ethylene polymerization. *Appl. Organomet. Chem.* **2022**, *36*, e6834. [CrossRef]

91. Zhang, P.; Zhao, M.; Pang, W.; Chen, C. Lewis acid/base modulation in β-diiminate zinc-catalyzed switchable ring-opening polymerization of rac-lactide. *Sci. China Chem.* **2019**, *62*, 475–478. [CrossRef]

92. Smith, A.J.; Kalkman, E.D.; Gilbert, Z.W.; Tonks, I.A. ZnCl₂ capture promotes ethylene polymerization by a salicylaldiminato Ni complex bearing a pendent 2,2′-bipyridine group. *Organometallics* **2016**, *35*, 2429–2432. [CrossRef]

93. Chiu, H.C.; Koley, A.; Dunn, P.L.; Hue, R.J.; Tonks, I.A. Ethylene polymerization catalyzed by bridging Ni/Zn heterobimetallics. *Dalton Trans.* **2017**, *46*, 5513–5517. [CrossRef] [PubMed]

94. Johnson, L.; Wang, L.; McLain, S.; Bennett, A.; Dobbs, K.; Hauptman, E.; Ionkin, A.; Ittel, S.; Kunitsky, K.; Marshall, W.; et al. Copolymerization of ethylene and acrylates by nickel catalysts. In *Beyond Metallocenes*; American Chemical Society: Washington, DC, USA, 2003; pp. 131–142.

95. Chiu, H.-C.; Pearce, A.J.; Dunn, P.L.; Cramer, C.J.; Tonks, I.A. β-oxo-δ-diimine nickel complexes: A comparison of tautomeric active species in ethylene polymerization catalysis. *Organometallics* **2016**, *35*, 2076–2085. [CrossRef]

96. Cai, Z.; Xiao, D.; Do, L.H. Fine-tuning nickel phenoxyimine olefin polymerization catalysts: Performance boosting by alkali cations. *J. Am. Chem. Soc.* **2015**, *137*, 15501–15510. [CrossRef]

97. Zhang, D.; Chen, C. Influence of polyethylene glycol unit on palladium- and nickel-catalyzed ethylene polymerization and copolymerization. *Angew. Chem. Int. Ed.* **2017**, *56*, 14672–14676. [CrossRef]

98. Ma, X.; Zhang, Y.; Jian, Z. Tunable branching and living character in ethylene polymerization using "polyethylene glycol sandwich" α-diimine nickel catalysts. *Polym. Chem.* **2021**, *12*, 1236–1243. [CrossRef]

99. Cai, Z.; Do, L.H. Customizing polyolefin morphology by selective pairing of alkali ions with nickel phenoxyimine-polyethylene glycol catalysts. *Organometallics* **2017**, *36*, 4691–4698. [CrossRef]

100. Tran, T.V.; Nguyen, Y.H.; Do, L.H. Development of highly productive nickel–sodium phenoxyphosphine ethylene polymerization catalysts and their reaction temperature profiles. *Polym. Chem.* **2019**, *10*, 3718–3721. [CrossRef]

101. Tran, T.V.; Karas, L.J.; Wu, J.I.; Do, L.H. Elucidating secondary metal cation effects on nickel olefin polymerization catalysts. *ACS Catal.* **2020**, *10*, 10760–10772. [CrossRef]

102. Tran, T.V.; Lee, E.; Nguyen, Y.H.; Nguyen, H.D.; Do, L.H. Customizing polymers by controlling cation switching dynamics in non-living polymerization. *J. Am. Chem. Soc.* **2022**, *144*, 17129–17139. [CrossRef]

103. Xiao, D.; Cai, Z.; Do, L.H. Accelerating ethylene polymerization using secondary metal ions in tetrahydrofuran. *Dalton Trans.* **2019**, *48*, 17887–17897. [CrossRef]

104. Wilders, A.M.; Contrella, N.D.; Sampson, J.R.; Zheng, M.; Jordan, R.F. Allosteric effects in ethylene polymerization catalysis. Enhancement of performance of phosphine-phosphinate and phosphine-phosphonate palladium alkyl catalysts by remote binding of $B(C_6F_5)_3$. *Organometallics* **2017**, *36*, 4990–5002. [CrossRef]

105. Cai, Z.; Do, L.H. Thermally robust heterobimetallic palladium–alkali catalysts for ethylene and alkyl acrylate copolymerization. *Organometallics* **2018**, *37*, 3874–3882. [CrossRef]

106. Tahmouresilerd, B.; Xiao, D.; Do, L.H. Rigidifying cation-tunable nickel catalysts increases activity and polar monomer incorporation in ethylene and methyl acrylate copolymerization. *Inorg. Chem.* **2021**, *60*, 19035–19043. [CrossRef]

107. Deacy, A.C.; Moreby, E.; Phanopoulos, A.; Williams, C.K. Co(III)/alkali-metal(I) heterodinuclear catalysts for the ring-opening copolymerization of CO_2 and propylene oxide. *J. Am. Chem. Soc.* **2020**, *142*, 19150–19160. [CrossRef] [PubMed]

108. Trott, G.; Garden, J.A.; Williams, C.K. Heterodinuclear zinc and magnesium catalysts for epoxide/CO_2 ring opening copolymerizations. *Chem. Sci.* **2019**, *10*, 4618–4627. [CrossRef]

109. Deacy, A.C.; Kilpatrick, A.F.R.; Regoutz, A.; Williams, C.K. Understanding metal synergy in heterodinuclear catalysts for the copolymerization of CO_2 and epoxides. *Nat. Chem.* **2020**, *12*, 372–380. [CrossRef]

110. Diment, W.T.; Gregory, G.L.; Kerr, R.W.F.; Phanopoulos, A.; Buchard, A.; Williams, C.K. Catalytic synergy using Al(III) and group I metals to accelerate epoxide and anhydride ring-opening copolymerizations. *ACS Catal.* **2021**, *11*, 12532–12542. [CrossRef]

111. Plajer, A.J.; Williams, C.K. Heterotrinuclear ring-opening copolymerization catalysis: Structure–activity relationships. *ACS Catal.* **2021**, *11*, 14819–14828. [CrossRef]

112. Saini, P.K.; Romain, C.; Williams, C.K. Dinuclear metal catalysts: Improved performance of heterodinuclear mixed catalysts for CO_2-epoxide copolymerization. *Chem. Commun.* **2014**, *50*, 4164–4167. [CrossRef]

113. Cai, Z.; Xiao, D.; Do, L.H. Cooperative heterobimetallic catalysts in coordination insertion polymerization. *Comments Inorg. Chem.* **2019**, *39*, 27–50. [CrossRef]